UC San Diego
Research Final Reports

Title

Mapping and Monitoring Large-Scale Ocean Fronts Off the California Coast Using Imagery from the GOES-10 Geostationary Satellite

Permalink

https://escholarship.org/uc/item/9mh4f40k

Authors

Breaker, Laurence C.
Mavor, Timothy P.
Broenkow, William W.

Publication Date

2005-04-18

Contents

Abstract

Despite their importance to fisheries management, environmental monitoring, search-and-rescue operations, and underwater sound, there is little readily available information on when and where oceanic fronts occur off the coast of California. To help fill this gap, scientists at Moss Landing Marine Laboratories, together with NOAA's National Environmental Satellite Data and Information Service (NESDIS), with support from California Sea Grant, have produced a series of monthly maps showing the locations of fronts off the California coast. They were created using remote sensing data from the GOES-10 geostationary satellite. A total of 48 frontal maps were produced on a monthly basis over the four-year period from July 2000 through June 2004. These maps are available from the following Internet address: http://physoce.mlml.calstate.edu/fronts/.

The sequence of maps shows that fronts initially develop near the coast, usually in March, when coastal upwelling begins. As coastal upwelling intensifies, the fronts gradually move offshore and by September they often extend several hundred kilometers from the coast. By November, frontal activity decreases significantly, reaching a minimum between December and February.

In an effort to validate the use of satellite data in mapping fronts, satellite-derived estimates of sea-surface temperature were compared to direct measurements of temperature taken during a California Cooperative Oceanic Fisheries Investigations' (CalCOFI) cruise. Agreement between the two independent sources of data, given the differences in resolution and timing, was encouraging.

A number of recommendations are made for improving the product. These include averaging or compositing the satellite data over periods of less than a month to better resolve the evolution and movement of fronts. Finally, it is recommended that a concerted effort be made to market this product to those who can most benefit from the information. The goal of this publication is to increase awareness of this source of information and to make the maps that have been produced available to potential users.

1. Introduction

a. Background

Oceanic fronts occur at the boundaries that separate different water masses, similar to their occurrence in the atmosphere where they separate different air masses. In the ocean, different water masses are characterized by different physical, biological and optical properties. According to Roden (1976), ocean fronts are regions of intensified motion, sharp gradients, decreased stability, and increased turbulence and convection.

In the oceanic case, because of their diverse nature, it is difficult to give a precise definition of ocean fronts (Fedorov 1983), although numerous attempts have been made. According to Owen (1981), for example, "a front is a line or linear zone that defines an axis of laterally convergent flow, below or above which vertical motion is induced." Frontal boundaries are often so pronounced that they are easily observed aboard ship with the naked eye. Fronts occur throughout the world's oceans on all scales, but many fronts are found in selected areas where their occurrence is favored by the prevailing atmospheric and oceanic conditions, and sometimes the bottom topography. Ocean fronts, although often observed at the surface, occur at all depths. In most cases, however, ocean fronts occur in the upper 1 km of the water column (Roden 1976). An important aspect of frontal behavior is how they form, intensify and dissipate over time (Roden and Paskausky 1978).

One of the most important aspects of ocean fronts is that they are characterized by convergent flow at the surface (Bowman 1978). For this reason, fronts are regions that are rich in biological productivity. Free floating biota are drawn into frontal zones due to the prevailing convergent flow, a process that in time can lead to a fully developed food chain as fish at higher trophic levels are likewise attracted to these regions in search of food.

Off the coast of California, several different types of ocean fronts occur. Near the coast, small scale fronts may be found that are associated with estuarine/river discharge. Near the coast in shallow water where the influence of bottom topography may be strong, fronts can be associated with major bathymetric features, particularly along the continental margin (Holladay and O'Brien 1975).

One cause of ocean fronts is coastal upwelling, where waters at depth are brought to the surface in response to the surface wind, which causes the surface waters next to the coast to diverge.

Coastal upwelling is a dominant physical process within 50 km of the coast between March and September when the alongshore winds are upwelling favorable, i.e., southward.

Further from shore, upwelled waters may be more the result of positive wind stress curl that leads to divergent flow near the ocean surface.

Fronts associated with coastal upwelling occur near the coast and then progressively move further offshore between March and September. As upwelling proceeds, the offshore transport of cold, upwelled water meets warmer waters that are displaced seaward. The interaction of the upwelled waters with the displaced, warmer waters forms a front. According to Mann and Lazier (1991), during an upwelling event, the front forms initially close to the coast and then moves offshore. At some distance, equilibrium is reached and the front ceases to move further offshore. At this point, the upwelled waters are driven downward beneath the offshore waters. Because upwelling fronts tend to slope in the same direction as the cross-shelf topography, they are often referred to as "prograde" fronts (Mooers et al. 1978). Breaker (1981) observed that maximum frontal activity most likely corresponds to periods of intense upwelling. The upwelling in turn is the result of strong, persistent southward wind stress and wind stress curl. During these periods, the major upwelling fronts may intensify and move further offshore.

On seasonal time scales, satellite observations have shown that the region primarily influenced by coastal upwelling gradually moves offshore between April and September. In the early spring the offshore extent of coastal upwelling may extend only ten or several tens of km offshore; whereas by September, areas influenced by cold, upwelled water may extend several hundred km offshore (Breaker and Mooers 1986). Upwelling at the coast continues throughout the upwelling season and produces secondary fronts that also migrate offshore. However, because these fronts are embedded in previously upwelled water, they are more difficult to detect.

Upwelling fronts are often characterized by strong thermal and salinity gradients. Because salinities are usually higher and temperatures lower on the inshore side of these fronts, strong density gradients are often produced that in turn lead to vigorous along-front flows that can penetrate to depths of 200 m (Armstrong et al. 1987). Along-front flows may act to redistribute the biota in these regions. According to Breaker (1981), upwelling fronts are often ephemeral—forming, intensifying and disappearing rapidly due to sudden changes in the surface wind field. According to Mooers et al. (1978), cross-frontal mixing enhances the exchange of nutrients in upwelling frontal zones, which may partly explain why well-developed food chains are often found on the seaward side of upwelling fronts. As a result, the width of the biologically productive zone can far exceed the width of the upwelling zone *per se* (Cushing

1971). Coastal upwelling fronts are also associated with differential vertical motions that bring nutrient-rich waters to the surface, providing another mechanism that concentrates marine life in these regions (Mooers 1978). Wave-like instabilities form along major upwelling boundaries that can lead to eddy formation (Breaker and Mooers 1986), providing yet another mechanism that could potentially concentrate marine life near frontal boundaries.

Beyond the region directly influenced by coastal upwelling (> ~ 50 km) lies the Coastal Transition Zone (Brink and Hartwig 1985), a region inhabited by long filaments of cold water that often originate closer to the coast and, in some cases, originate at coastal capes that may serve as upwelling centers. These features were first identified in satellite imagery in the late 1970s. They possess frontal boundaries that separate them from the surrounding offshore waters.

Far offshore in the California Current during the winter, fronts occur that are not related to upwelling and thus are due to other factors. Owen (1981) refers to these features generally as deep-sea fronts. They are most likely related to surface wind forcing and/or current interactions. In some cases, where dramatic changes in bottom depth occur, such as along the Mendocino Ridge or near major coastal submarine canyons, co-located fronts may be topographically related.

Interest in ocean fronts has increased in the last few years, at least in the ocean research community, as indicated by a special session devoted to this topic at the American Geophysical Union's Ocean Sciences Meeting in 2000 in San Antonio, Texas (Belkin and Spall 2002). One of the primary results of this meeting was the recognition that new developments in technology such as the Autonomous Underwater Vehicle (AUV) have made it possible to sample fronts on the scales that are required. Also, higher resolution ocean models have made it possible to more accurately predict the evolution and fine-scale structure of ocean fronts. The results of this meeting have been published in special issues on ocean fronts in *Dynamics of Atmospheres and Oceans*, and the *Journal of Marine Systems*.

Because of the contrasts in temperature and ocean color associated with ocean fronts, they can often be identified in high-resolution infrared (IR) and ocean color satellite imagery. As early as the mid-1970s it became apparent that high-resolution IR satellite imagery was useful in detecting ocean fronts off California (Bernstein et al. 1977). Several programs were conducted during the 1970s and 1980s to assist commercial fishermen in locating ocean fronts using imagery from the Very High Resolution Radiometer (VHRR), the Advanced Very High Resolution Radiometer (AVHRR), and the Coastal Zone Color Scanner (CZCS). These programs once again emphasized the

utility of satellite imagery to detect and track ocean fronts in California coastal waters (Breaker 1981; Montgomery et al. 1986). In the last 15 years, new automated techniques have been developed to detect ocean fronts using imagery primarily from the AVHRR (Cornillon and Watts 1987; Holyer and Peckinpaugh 1989; Cayula and Cornillon 1992; Cornillon and Cayula 1995; Ullman and Cornillon 2000; Mavor and Bisagni 2001).

b. Motivation

Most of the information on ocean fronts today appears in journal publications, and as a result is not readily available to many who may have a need for it. Also, because ocean fronts change in time and space and since we cannot predict their behavior in detail, monitoring ocean fronts from space on a regular basis should benefit the marine community, including a number of agencies. The National Marine Fisheries Service (NMFS), because of its fisheries management responsibility, could benefit from such a program because it would give them information on where fishing activity would most likely be expected to occur.

The Pacific Fisheries Environmental Laboratory of the NMFS in Monterey also provides information on ocean properties and processes that are related to fisheries. We believe that the work conducted during this project contributes directly to their mission by providing an important resource for fisheries and environmental research. The California Department of Fish and Game could also use information on ocean fronts to assist them in their management responsibilities for the marine environment. The U.S. Coast Guard conducts search and rescue missions in U.S. coastal waters, plus they have an environmental responsibility for providing a rapid response to oil spills. As such, information on ocean fronts could be of considerable benefit to the Coast Guard. Because the U.S. Environmental Protection Agency has the responsibility to monitor environmental conditions in U.S. coastal waters, this agency should likewise have an interest in this activity. The U.S. Navy's Fleet Numerical Meteorology and Oceanography Center (FNMOC) should have a strong interest in monitoring ocean fronts because of their responsibility for ocean environmental monitoring.

Ocean fronts also strongly influence underwater sound and may act as acoustical waveguides (Belkin 2002). During the early stages of this project, the CalCOFI Program expressed an interest in frontal mapping since it would assist researchers at sea in locating frontal regions that affect the distribution of physical and biological properties along the track lines that are sampled on a regular basis.

Since the original proposal was written, a new application for information on ocean fronts has emerged related to

ocean habitat mapping. It has long been known that different biota and species of fish are often found on opposite sides of major ocean fronts. A classic example off the coast of California relates to the salmon and albacore tuna fisheries. Salmon are found on the cold inshore side of major upwelling fronts, whereas tuna are found on the warm, offshore side. Within NOAA, and elsewhere around the world, there is growing interest in mapping various benthic and pelagic habitats in an effort to better manage the oceans.

This ambitious task has primarily involved marine geologists and marine biologists/ecologists up to this point, but in Australia the need for information on ocean fronts to complete any habitat mapping program has been recognized (G. Greene, personal communication). Including ocean fronts as part of habitat mapping is expected to take on added importance as the emphasis shifts from benthic to pelagic fisheries in this country in the near future.

c. The project and its goals

The primary goal of this project has been to provide information on the expected locations of major frontal boundaries off the California coast on a monthly basis using imagery from the GOES-10 geostationary satellite, and to make it readily available to a wide range of users. As a secondary goal, it was originally intended to use ocean color imagery from SeaWiFS to supplement the coverage from GOES to provide higher spatial resolution near the coast and during the Davidson Current period (November–February), when the gradients in sea-surface temperature (SST) are expected to be weak. However, after initial efforts to obtain useful data from the SeaWiFs archive at NASA, it became clear that we simply could not obtain clear sky coverage frequently enough to support the goals of this project. As a result, the imagery from GOES-10 has been used throughout the year. Also, as we have learned during the course of this project, frontal activity off the California coast, although generally weak and far offshore during the winter, does occur, and as a result, the imagery from GOES-10 was useful during this period. Although the duration of the project was for three years, it was our intent to utilize past coverage from the GOES-10 satellite to extend our results back in time to create a monthly sequence that spanned a period longer than three years, and possibly up to five years. As it turns out, the final sequence spans a four-year period from July 2000 through June 2004.

It was our primary goal to produce frontal maps that depict the expected locations of fronts off the coast of California on a monthly basis from about 30° to 40°N and out to at least 125°W. Our final product dimensions are from 30° to 43°N, and out to 128°W. This area encompasses the primary

upwelling zone off California, where frontal development is most pronounced, and the main body of the California Current, where deep-sea fronts occur. These results are presented in section 3a. Also, it was our intent to distribute the monthly frontal maps over the Internet. The maps are presently available at: http://physoce.mlml.calstate.edu/fronts/. Finally, we wanted to validate the occurrence and location of fronts as depicted in the imagery from GOES-10 through comparisons with *in situ* data collected aboard ship during selected CalCOFI cruises.

2. The Approach

Maps of ocean fronts off the California coast have been produced using IR imagery from the imager on the GOES-10 geostationary satellite. An illustration of the GOES satellite is shown in Figure 1. The imager on GOES-10 has 4 km resolution in the IR channels, offering improved spatial resolution compared to data from previous geostationary satellites (Menzel and Purdom 1994). This higher spatial resolution is particularly advantageous in detecting ocean fronts, which characteristically have relatively small spatial scales in the cross-frontal direction. However, of equal importance, this satellite, because of its geostationary orbit, can acquire images as often as every half-hour, providing far more opportunities to obtain cloud-free coverage of the study area than could be acquired from polar-orbiting satellites. With respect to the California coast, persistent cloud cover has severely limited the utility of polar-orbiting satellite coverage during the spring and summer when coastal upwelling occurs.
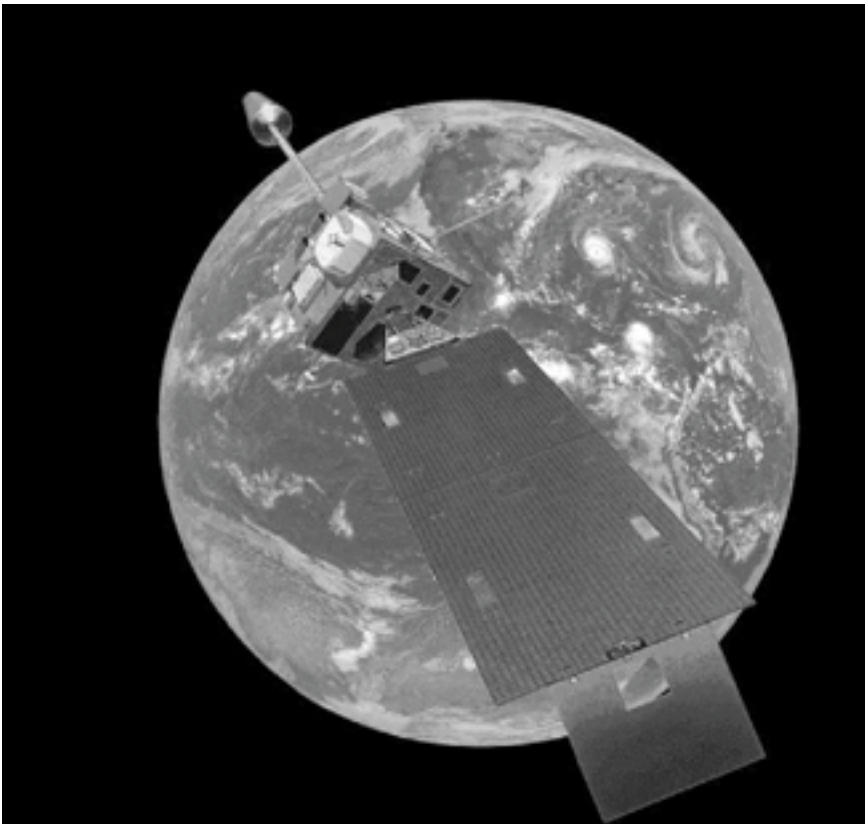
Figure 1. An artist's rendition of the GOES geostationary satellite.

The GOES-10 geostationary satellite is positioned above the equator at 135°W, providing spatial coverage of a region that extends from 45°S to 60°N, and from 90°W to 180°W. Hourly derived sea-surface temperatures (SSTs) from the GOES satellites, operated by NOAA/NESDIS, became routinely available in 2000. Multi-channel brightness temperatures at 3.9, 11, and 12 microns are retrieved from the imager on the GOES satellites, using an operational algorithm to produce SST fields on an hourly basis at approximately 5 km resolution. Utilization of the various wavelengths in the multi-channel SST and cloud-screening algorithms produces SST retrievals with acceptable accuracy when compared to buoy observations. By using a multi-channel retrieval algorithm, the effects of atmospheric moisture are also removed.

A cloud screening algorithm using the multi-channel approach of Wu et al. (1999) is used to identify picture elements (pixels) in the image that are obscured by cloud. Cloud clearing based on the warmest-pixel method is used to eliminate clouds colder than the underlying SST for any period over which the images are combined. However, marine stratus along the California coast is often similar in temperature to the underlying SST, and thus the influence of cloud cover may not always be removed. The primary advantage of the GOES SST retrievals over SSTs retrieved from polar-orbiting satellites is the temporal frequency of coverage: each location is observed 24 times per day, compared to twice per day from a single polar-orbiting satellite. While regions that are persistently cloud-covered may not benefit greatly from this increased observation frequency, the possibility of inferring cloud-free SSTs at least once each day is significantly increased.

A first step in the frontal analysis is based on the calculation of daily-averaged SST fields for the study area starting in June 2000, when the current SST algorithm was first implemented. After cloud screening, a daily-averaged GOES SST field is calculated, based on 24 hourly GOES SST fields that are processed each day. At each pixel location, the mean SST is calculated from the valid SST retrievals extracted from the 24 hourly fields. Additionally, the total number of valid SST retrievals extracted from these fields is determined for each pixel. As a result, the statistical significance of the mean SST field can be calculated. GOES SST fields are then processed by an edge-detection algorithm to identify SST fronts.

A gradient-based algorithm is used for each of the daily-averaged SST fields, employing a threshold to retain regions that exhibit gradients greater than 0.375°C per pixel, and then selectively thinning those regions to obtain a single front. A standard gradient operator is used to estimate the magnitude of the gradients in SST (e.g., Richards 1986). For each frontal image, we take the number of times a particular pixel qualifies

as a front and divide this value by the number of times that the pixel was clear during that time period, yielding a Probability of Frontal Encounter, or PFE. Where regions of a frontal map are relatively dark, the PFE is high, and vice versa. However, it is possible, although unlikely, that regions portrayed in white may still have fronts, or high PFEs; but instead, the region was completely cloud covered at all times. After these steps are completed, a time-series of daily frontal images is obtained.

By combining the detected fronts for various time periods, preferred locations of frontal activity are revealed. The process of combining the sequence of images that enter into the analysis is called compositing. It is a powerful technique for reducing the influence of cloud contamination but has several limitations. First, although the effectiveness of image compositing improves as the window length is increased, interpretation of the results is more difficult because image composites do not provide synoptic views of the ocean during periods when the fields of interest may be changing. When this occurs, the areas of frontal activity become smeared or blurred over the compositing interval. In general, the number of cloud-free observations at each pixel location will be different and so the temperature field that is produced is not statistically homogeneous (Adams and Breaker 2003).

Finally, monthly maps of frontal probability are produced that are displayed on a latitude-longitude grid. Because of the processing methods employed, it was not possible to extract frontal activity within the first 30 km of the coast, so the final product simply shows a front-free, i.e., clear, region next to the coast.

Dissemination of the product has been via the Internet. The monthly frontal analyses were produced by NOAA/NESDIS and originally displayed on their Web site: http://manati.orbit. nesdis.noaa.gov. They are now available at http://physoce.mlml. calstate.edu/fronts/.

A related goal of this project was to compare the satellite-derived frontal analyses with *in situ* data where such comparisons could be made. The study area includes the standard grid of CalCOFI stations, so it was possible to make several comparisons between selected frontal analyses and sea-surface temperatures collected aboard ship during a CalCOFI cruise in November 2002. These results are presented in section 3b.

3. Results

a. Analysis of the frontal maps

Between July 2000 and June 2004, 48 monthly frontal maps were produced. All maps are included on the enclosed CD-ROM. To illustrate certain points, we initially present several maps for discussion. We then summarize our findings based on the entire sequence. In the following discussions, although the Probability of Frontal Encounter (PFE) has a rather precise definition, we use the subjective terms "frontal activity" and "frontal band" frequently. Frontal activity implies relatively high PFEs (i.e., darker regions), but the associated frontal patterns may appear rather disorganized. When we refer to a frontal band, the PFEs are again relatively high, but the pattern appears to be more spatially organized.

Figure 2 shows the frontal map for August 2000. The frontal loci are well-defined in this case, with frontal activity extending in a band more or less parallel to the coast out to at least 200–300 km offshore.
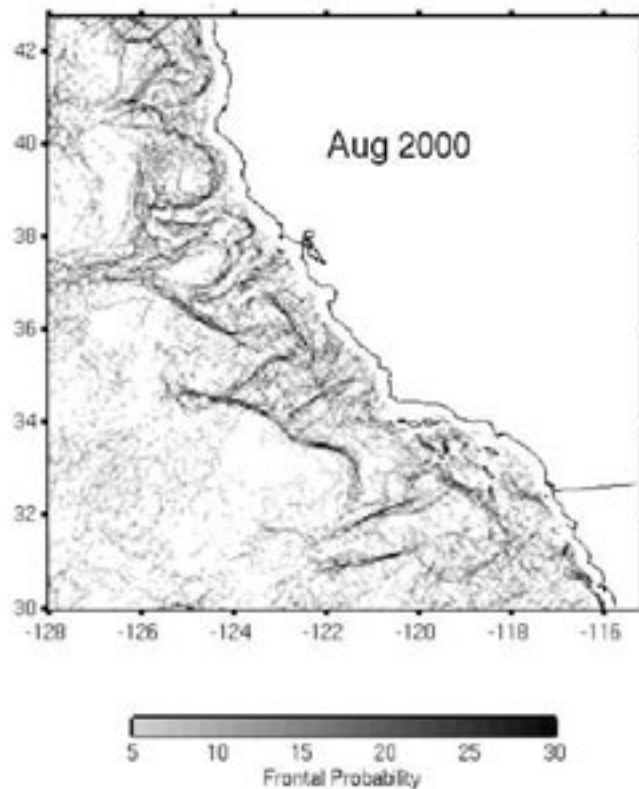
Figure 2. Frontal map for August 2000.

The curvature of the coastline from San Francisco north is reflected in the frontal patterns. It is particularly apparent between Cape Blanco (~38.5°N) and Cape Mendocino (~40°N), where dynamic heights from CalCOFI have frequently depicted an anticyclonic eddy with similar dimensions (Wyllie 1966). West of 126°W at ~37°N, weaker frontal loci are most likely associated with upwelling filaments that previously originated closer to the coast.

A frontal map for February 2001 is shown in Figure 3. Virtually no frontal activity is seen near the coast, and for the most part, further offshore. In the years included in the sequence, less frontal activity occurs during January and February near coast and offshore than during the rest of the year. This is undoubtedly due to the prevailing winds which are generally weak and variable between December and March, particularly between Point Conception and Cape Mendocino (Nelson 1977).
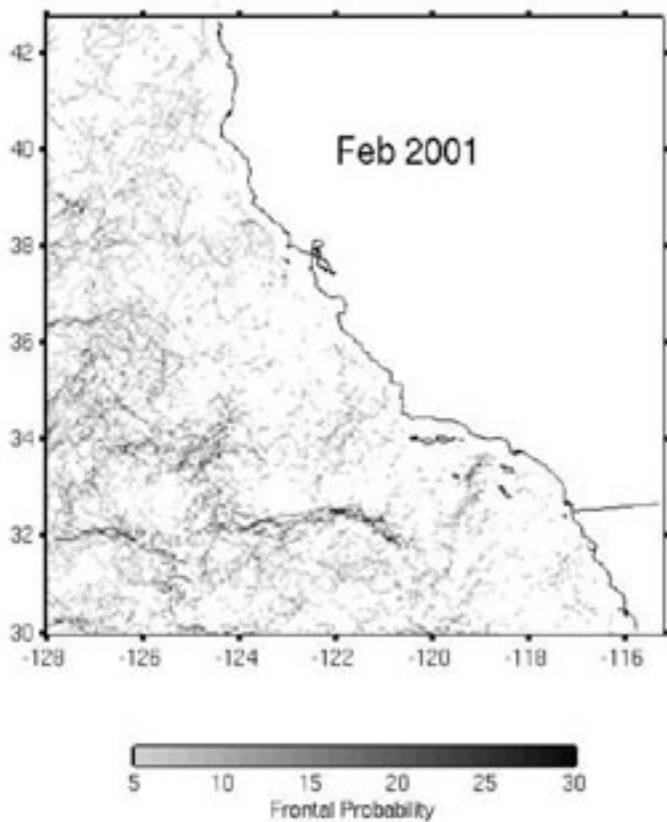

Figure 3. Frontal map for February 2001.

Figure 4 shows a frontal map for April 2001. Frontal activity is concentrated primarily within the first 50 km of the coast far to the south (< 33°N), and further north between Point Conception (~34.5°N) and Cape Blanco (~38.5°N), consistent with the early stages of coastal upwelling that often starts in March. In 2001, however, no upwelling activity was apparent along the coast in March as it was during the other years in the sequence. Except south of 34°N, little or no organized frontal activity occurs beyond ~100 km from the coast.
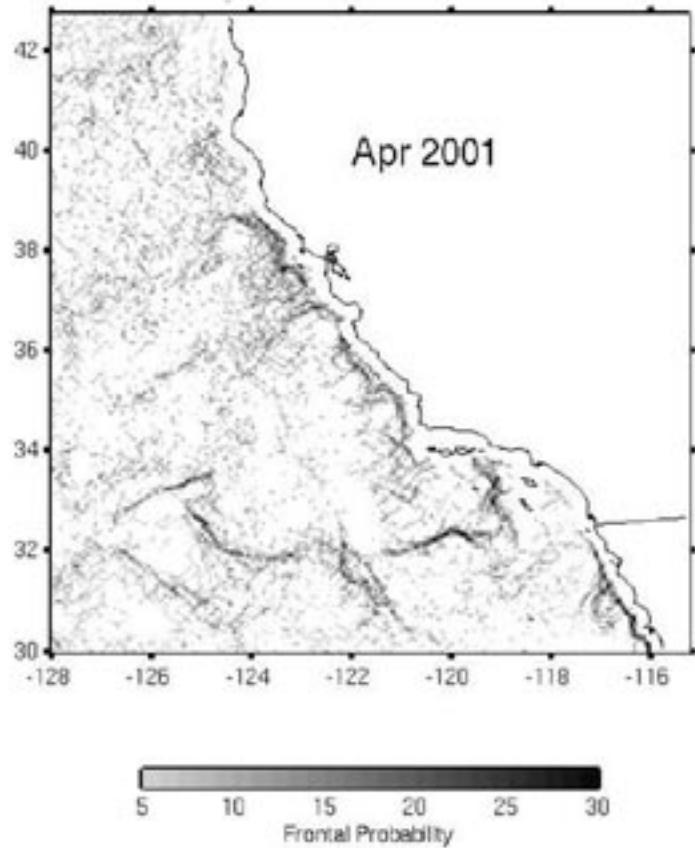
Figure 4. Frontal map for April 2001.

The frontal map in Figure 5 for June 2002 depicts frontal activity near the coast related to coastal upwelling north of Point Conception, and further offshore where frontal bands appear that are more or less perpendicular to the coast, consistent with extended filaments of cold upwelled water located in the Coastal Transition Zone. Even further offshore several fronts can be seen that are most likely deep-sea fronts and thus not related to coastal or offshore upwelling. We also note two parallel frontal bands approximately 30 km apart north of Cape Mendocino that are most likely the result of episodic upwelling separated in time by several weeks. Finally, rather disorganized frontal activity occurs in the Southern California Bight and over the adjacent continental borderland that could be related to the local bathymetry. Based on the entire sequence, frontal activity is often observed in this area.

A frontal map for November 2003 (Figure 6) shows frontal activity near the coast between 35°N and 39°N and extending far offshore. Further south (32°N–34°N), frontal activity is also seen far offshore. By November, frontal activity is not usually apparent near the coast since upwelling has essentially ceased, and so this map is not necessarily representative of this period. However, during November major activity often occurs much further offshore that may, in some cases, represent remnants of upwelling filaments.
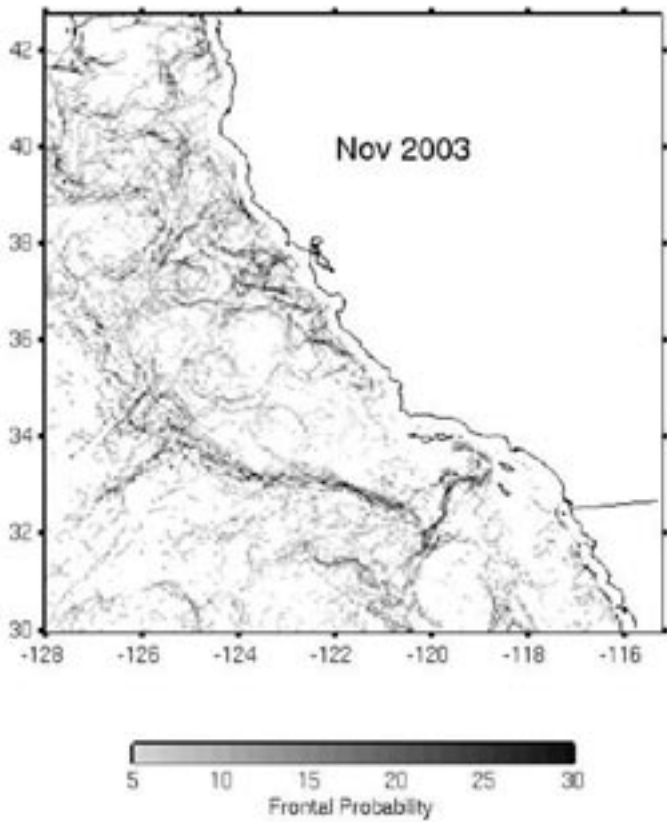
Figure 5. Frontal map for June 2002.

Figure 6. Frontal map for November 2003.

The frontal maps clearly indicate strong seasonal patterns. During January and February, virtually no frontal activity associated with coastal upwelling occurs along the California coast. However, farther offshore in the main body of the California Current occasional deep-sea fronts may occur. Starting in March, generally weak but discernible coastal upwelling, as indicted by weak frontal activity within the first 50 km of the coast, occurs starting at Point Conception or further south, progressing north in April and May. By April, fronts associated with coastal upwelling become well-developed although they are usually found less than 100 km from the coast. Fronts that are most likely not related to upwelling may also occur further offshore.

During May, coastal and offshore upwelling, as indicated by strong frontal activity, is observed along the entire coast from Point Conception north. Upwelling filaments frequently oriented perpendicular to the coast begin to appear farther offshore. Frontal activity related to coastal and offshore upwelling appears to be most intense during June, consistent with the maximum, upwelling-favorable (southward, parallel to the coast) wind stress that occurs at this time. Upwelling-related frontal activity may occur several hundred km offshore in June. During July and August, upwelling-related frontal activity extends even further offshore, out to 200–300 km from the coast. During September and into October, upwelling-related frontal activity reaches its maximum extent offshore, often out to 400 km or more. During November, frontal activity is observed far off the coast but has started to weaken as the winds become more variable. Remnants associated with previous upwelling may still appear far offshore. Finally, by December, frontal activity has become still weaker and less well defined, with almost no trace of frontal activity near the coast.

Frontal bands tend to parallel the coast within the first 100 km or so offshore. Further offshore, frontal activity can be oriented in any direction, but between about May and October there are fronts possibly associated with upwelling filaments that are oriented roughly perpendicular to the coast. Overall, frontal loci further offshore do not repeat themselves from one month to the next or from one year to the next during the same month.

Frontal activity in the Southern California Bight, although often significant, tends to be disorganized in comparison to the more distinct frontal bands that are observed further offshore. There is no obvious relationship between frontal activity and climatological wind stress curl over the California Current (Nelson 1977), but this could reflect major differences between the climatological and instantaneous values of this derived parameter. It is not clear exactly what role cloud cover plays in influencing the clarity of the frontal activity being

portrayed. Beyond the continental margin, little or no relationship to the underlying bathymetry could be found with the possible exception of the Mendocino Ridge, a major escarpment oriented in the east-west direction extending off Cape Mendocino, and the Monterey Submarine Canyon, located in Monterey Bay and extending offshore. On occasion, frontal bands appear to form around the edges of the Canyon forming a horseshoe pattern with the open end located to the west. This feature has been observed in individual satellite images. Even though the cloud-clearing algorithm may be effective, intermittent gaps in frontal coverage may still occur that detract from the analysis. Finally, because of the frequency of coverage obtained using the imagery from GOES-10 (24 images per day), it has been possible to obtain information on the occurrence and persistence of ocean fronts that would have been impossible to obtain from polar-orbiting satellites.

b. Comparison with *in situ* observations

As part of this project it was one of our goals to compare the monthly composited frontal maps with *in situ* temperature data collected aboard ship during selected CalCOFI cruises. As it turned out, it was very difficult to find suitable underway temperature data collected during the seasonal CalCOFI cruises that could be directly compared with the frontal maps. Either the *in situ* observations were available in areas where there were no fronts or, where fronts occurred, there were no coincident shipboard data. Finally, one month was found—November 2002—where well-defined frontal activity and shipboard temperature data were both available.

A CalCOFI cruise in the vicinity of line 67 off Central California was conducted during November 2002. The ship's track is shown in Figure 7, superimposed on the frontal map for November 2002. The track is made up in part of four lines running more or less perpendicular to the coast. To provide a measure of distance, the maximum distance offshore for the top line is approximately 260 km. The measurements of SST were made using an underway thermalsalinograph. Salinities were also examined, but SST is used here for comparison. The observations were made between November 12 and 18, 2002, and thus were concentrated toward the middle of the month. Line segments have been chosen to coincide with well-defined frontal bands that are clearly depicted in Figure 7.

Figure 8 shows the specific line segments. Line 1 and Line 2, together, span the top trackline in Figure 7 and starts at the coast. Line 3 spans a distance of 90 km along the bottom trackline, whose location along the track can be identified by its unique saw-toothed pattern, and begins offshore and heads toward the coast. Line 4 (120 km) can also be located by its saw-toothed pattern along the third trackline in Figure 7,
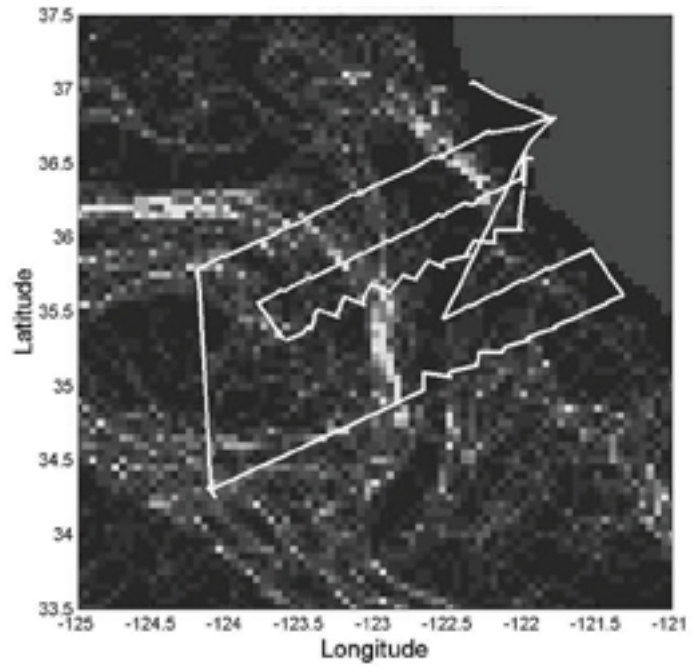
Figure 7. Probability map of frontal encounter from GOES-10 for November 2002 with ship track superimposed.
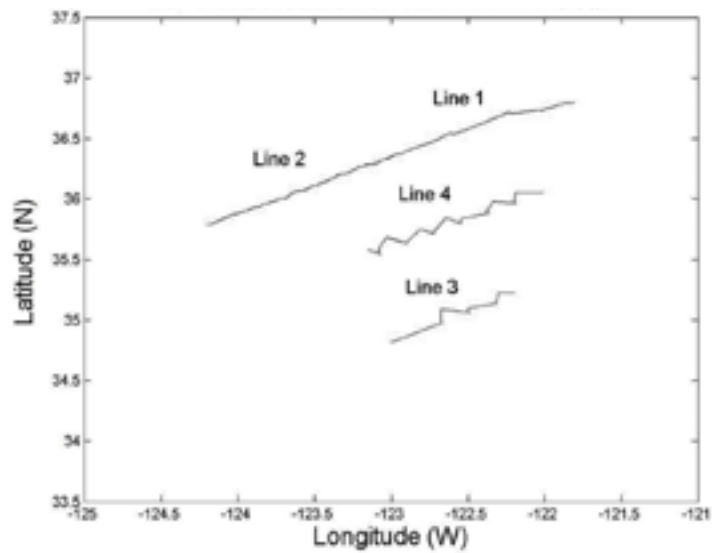

Figure 8. Ship track sections where frontal encounters occurred.

and likewise is directed from offshore toward the coast. In the interest of brevity, we only show 3 of the 4 trackline comparisons that were made: Lines 1, 2 and 3.

What we hope to find are cases where sudden and relatively large changes in temperature (≥ 1–2°C over distances of ≤ 5–10 km) coincide with higher values of the PFE (≥ 15). The scales for SST (solid lines) and PFE (asterisks in Figures 9–11*) are completely independent and have been plotted separately at each end of the figures in question.

We should not necessarily expect close agreement for

*The symbols representing the PFEs in Figures 9–11, although somewhat blurred, are referred to in the text as asterisks.
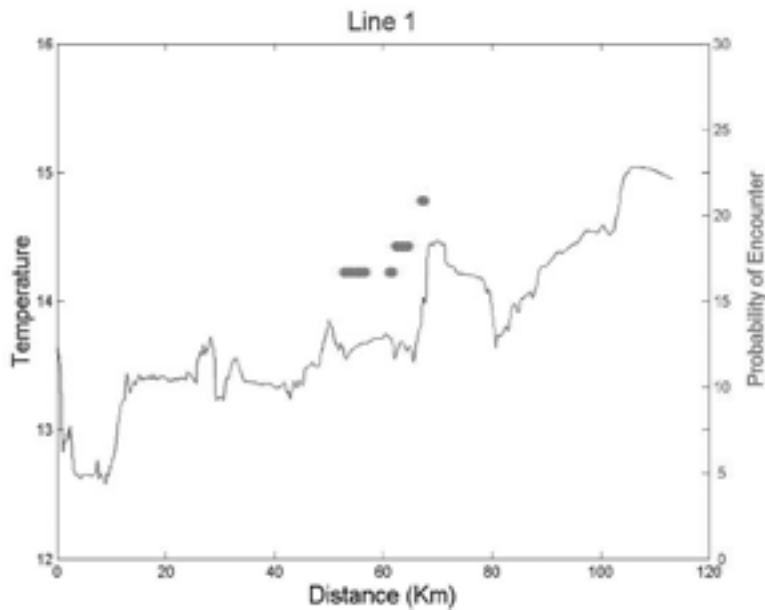
Figure 9. Comparison of Line 1.

several reasons. First, the maps are produced over a period of a month, whereas the shipboard data were collected over a period of only a week or two toward the middle of the month. Second, the PFEs are spatially averaged yielding a resolution of 5 km, far less than the resolution of the underway data.

Figure 9 compares the PFE with SST over a distance of ~120 km. A slight increase in PFE does, in fact, occur at a distance of approximately 65 km from the origin (the coast in this case). The feature associated with the higher PFE can easily be seen in the frontal map itself (see Figure 7) as a relatively bright band that intersects the trackline midway along its course.

In Figure 10, the comparison for Line 2 is shown. In this case the agreement is apparently poor. However, the high value of PFE at 80 km could be related to the abrupt change in SST that occurs between 40 and 50 km offshore, if allowance is made for a possible shift in the frontal position during the month. Line 3 in Figure 11 actually shows relatively good agreement between SST and the PFE at a distance of approximately 15 km from the origin (offshore, in this case), where a PFE of ~20 corresponds to a decrease in temperature of almost 2°C over a distance of ~10 km. The corresponding frontal band can again be seen in Figure 7. Finally, the comparison for Line 4, although not shown, is similar to Line 3 in that the same frontal band (i.e., locus of relatively high PFEs) crosses both tracklines. Overall, we find the comparisons between the *in situ* temperature data and the satellite-derived frontal probabilities encouraging, although differences in the temporal and spatial resolutions are a detraction.
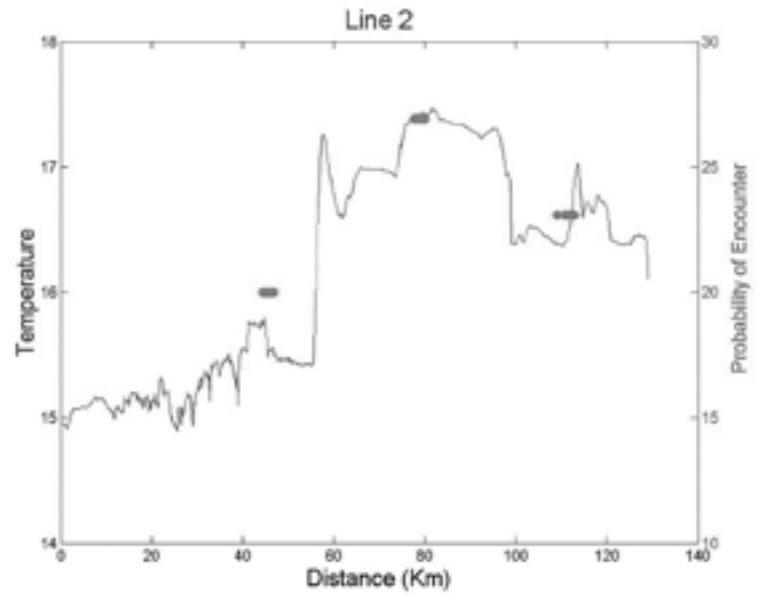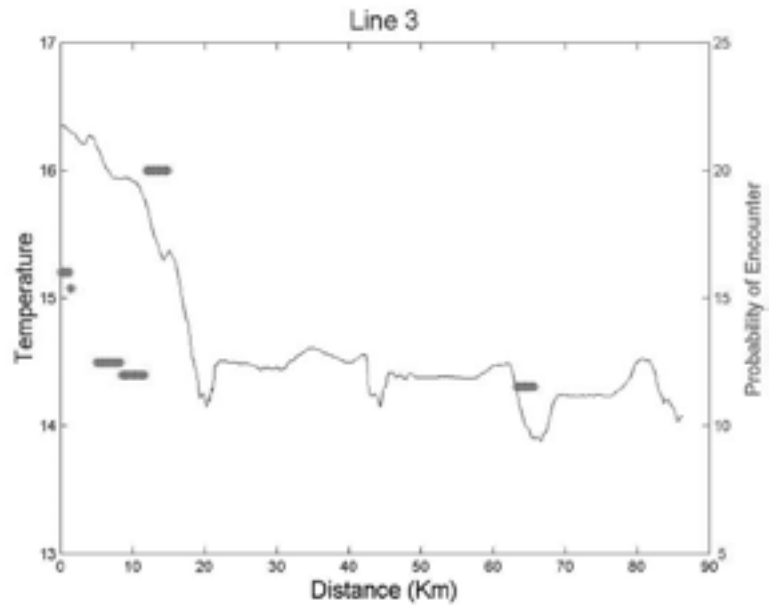
Figure 10. Comparison of Line 2.

Figure 11. Comparison of Line 3.

4. Problems and Recommendations

Several problems were encountered during the course of the project. First, as the sequence of frontal maps evolved, it became clear that during part of the year a monthly window is probably too long. During the winter between November and February, monthly composites appear to be satisfactory. However, during the spring, as coastal upwelling intensifies and spreads offshore, maps produced on a shorter time scale might capture more of the changes in frontal evolution that take place, thus reducing any smearing of the frontal patterns.

We recommend that window lengths of roughly two weeks be tried and compared with the existing monthly window to see what improvements in frontal resolution and clarity might be achieved. The tradeoff, of course, is that for shorter compositing windows, the number of cloud-free views of the ocean surface are reduced and, accordingly, the statistical confidence of the values of PFE that are produced.

Second, the region nearest the coast, i.e., the first 30 km, as explained earlier, is not covered in the present frontal analyses. This is a region of considerable interest where frontal activity is expected to be relatively intense primarily due to coastal upwelling. Although it will not be possible to completely solve this problem because the pixels closest to the coast are contaminated by land, the resolution of the analysis could be increased from 5 km, to approximately 2 or 3 km, thus reducing the size of this region.

Although it was our hope that frontal maps could be produced in near real time, it was not possible to accomplish this objective in many cases. We believe that the utility of this product could be greatly enhanced if it could be produced in closer to real time.

Finally, one of the most serious omissions during the project was a lack of marketing. We firmly believe that there are many potential users of this product who were simply not aware of its availability. We strongly recommend that if NOAA/NESDIS decides to produce this product on an operational basis in the future, a concerted effort be made to alert the marine community to its existence.

5. Points of Contact

Laurence C. Breaker
Moss Landing Marine Laboratories
8272 Moss Landing Road,
Moss Landing, CA 95039
Phone: (831) 771-4498   Email: Lbreaker@mlml.calstate.edu

Marsha Gear
California Sea Grant College Program
9500 Gilman Drive, Dept. 0232
La Jolla, CA 92093
Phone: (858) 534-0581   Email: mgear@ucsd.edu

William G. Pichel
NOAA/NESDIS
Route: E/RA3
NOAA Science Center
Camp Springs, MD 20746
Phone: (301) 763-8231   Email: william.g.pichel@noaa.gov

6. Acknowledgments

7. References

Adams, J. and L. Breaker, 2003. Sanctuary "hot spots." Satellite observations of ocean fronts and their composite histories in and beyond the Monterey Bay National Marine Sanctuary. Monterey Bay National Marine Sanctuary Symposium, Fort Ord, California.

Armstrong, D.A. et al., 1987. Physical and biological features across the upwelling front in the southern Benguela. In: The Benguela and Comparable Ecosystems. Eds. A. Payne, J. Gulland and K. Brink, Sea Fisheries Research Institute, Cape Town, pp. 171–190.

Belkin, I.M , 2002. New challenge: ocean fronts (Preface). *J. Mar. Sys*. 37:1–2.

Belkin, I.M. and M. Spall, 2002. New old frontier: ocean fronts (Editorial). *Dyn. Atmos. Oceans* 36:1–2.

Bernstein, R.L., L.C. Breaker, and R. Whritner, 1977. California current eddy formation: ship, air, and satellite results. *Science* 195:353–359.

Bowman, M.J.,1978. Oceanic Fronts in Coastal Processes. In: Oceanic Fronts in Coastal Processes. Eds. M. Bowman and W. Esias. Springer-Verlag, Berlin, pp. 2–5.

Breaker, L.C., 1981. The application of satellite remote sensing to west coast fisheries. *Mar. Technol. Soc*. 15:32–40.

Breaker, L.C. and C.N.K. Mooers, 1986. Oceanic variability off the central California coast. *Prog. Oceanog*. 17:61–135.

Brink, K.H. and E.O. Hartwig, 1985. Office of Naval Research Coastal Transition Zone Workshop Report. Naval Postgraduate School, Monterey, California, 67 pages.

Cayula, J.-F. and P. Cornillon, 1992. Edge detection algorithm for SST images. *J. Atmos. Oceanic Technol*. 9:67–80.

Cayula, J.-F. and P. Cornillon, 1995. Multi-image edge detection for SST images. *J. Atmos. Oceanic Technol*. 12:821–829.

Cornillon, P.C. and D.R. Watts, 1987. Satellite thermal infrared and inverted echo sounder determinations of the Gulf Stream northern edge. *J. Atmos. Oceanic Technol*. 4:712–723.

Cushing, D.H., 1971. Upwelling and the production of fish. *Adv. Mar. Biol*. 9:255–334.

Fedorov, K.N., 1983. The Physical Nature and Structure of Oceanic Fronts. Springer-Verlag, Berlin, 333 pages.

Holladay, C.G. and J.J. O'Brien, 1975. Mesoscale variability of sea surface temperature. *J. Phys. Oceanogr*. 5:761–772.

Holyer, R.J. and S.H. Peckinpaugh, 1989. Edge detection applied to satellite imagery of the oceans. *IEEE Trans. Geosci. Remote Sens*. 27:46–56.

Mann, K.H. and J.R.N. Lazier, 1991. Dynamics of Marine Ecosystems: Biological-physical Interactions in the Oceans. Blackwell Scientific Publications, Oxford, 466 pages.

Mavor, T.P. and J.J. Bisagni, 2001. Seasonal variability of sea-surface temperature fronts on Georges Bank. *Deep-Sea Research II*, 48:215–243.

Menzel, W.P. and J.F.W. Purdom, 1994. Introducing GOES-I: The first of a new generation of Geostationary Operational Environmental Satellites. *Bull. Amer. Meteor. Soc.* 75:757–781.

Montgomery, D.R., R.E. Wittenberg-Fay, and R.W. Austin, 1986. The applications of satellite-derived ocean color products to commercial fishing operations. *Mar. Technol. Soc.* 20:72–86.

Mooers, C.N.K., Flagg, C.N., and W.C. Boicourt, 1978. Prograde and retrograde fronts. In: Oceanic Fronts in Coastal Processes. Eds. M. Bowman and W. Esias. Springer-Verlag, Berlin, pp. 43–58.

Mooers, C.N.K., 1978. Oceanic fronts: a summary of a Chapman Conference. *EOS* 59:484–491.

Nelson, C.S., 1977. Wind stress and wind stress curl over the California Current. NOAA Technical Report NMFS SSRF-714, U.S. Dept. of Commerce, 87 pages.

Owen, R.W., 1981. Fronts and eddies in the sea: mechanisms, interactions and biological effects. In: Analysis of Marine Ecosystems. Academic Press, London, pp.197–233.

Richards, J.A., 1986. Remote Sensing Digital Image Analysis: An Introduction. Springer-Verlag, Berlin.

Roden, G.I., 1976. On the structure and prediction of oceanic fronts. *Naval Res. Rev.* 29:18–35.

Roden, G.I. and D.F. Paskausky, 1978. Estimation of rates of frontogenesis and frontolysis in the North Pacific Ocean using satellite and surface meteorological data from January 1977. *J. Geophys. Res.* 83:4545–4550.

Ullman, D.S. and P.C. Cornillon, 2000. Evaluation of front detection methods for satellite-derived SST data using *in situ* observations. *J. Atmos. Oceanic Technol.* 17:1667–1675.

Wu, X., W.P. Menzel, and G.S. Wade, 1999. Estimation of sea surface temperature using GOES-8/9 radiance measurements. *Bull. Amer. Meteorol. Soc.* 80:1127–1138.

Wyllie, J.G.1966. Geostrophic flow of the California Current at the surface and at 200 meters. California Cooperative Oceanic Fisheries Investigations Atlas No. 4.